Available online at www.sciencedirect.com
ScienceDirect
Proceedings of the Combustion Institute 32 (2009) 2583–2590
Proceedings of the Combustion Institute
www.elsevier.com/locate/proci

Effect of fuel type on the extinction of fuel and air stream diluted partially premixed flames

Andrew Lock [a,*], Suresh K. Aggarwal [b], Ishwar K. Puri [c]

[a] National Institute of Standards and Technology, Fire Research, 100 Bureau Dr. (Stop 8663), Gaithersburg, MD 20899, USA
[b] University of Illinois at Chicago, Chicago, IL, USA
[c] Virginia Polytechnic Institute and State University, Blacksburg, VA, USA

Abstract

Previous investigations have demonstrated that the roles of fuel stream dilution (FSD) and air stream dilution (ASD) in suppressing CO_2-diluted methane flames are strongly influenced by the level of partial premixing. Herein, we compare this influence for both counterflow and coflow laminar non-premixed and partially premixed flames (PPFs) established with various fuels, including methane, ethylene and acetylene. We find that ethylene and acetylene flames are more difficult to extinguish than those burning methane. For methane, FSD is more effective in suppressing PPFs while ASD suppression is more effective for non-premixed flames (NFs). In contrast, FSD suppression is typically more effective than with ASD for the corresponding ethylene and acetylene flames irrespective of the level of partial premixing. ASD is ineffective in suppressing the investigated coflow ethylene and acetylene flames. For counterflow flames, FSD is more effective in suppressing PPFs while ASD is more effective in suppressing NFs irrespective of the fuel burned but the range of equivalence ratios for the relative effectiveness of FSD and ASD depends strongly on the fuel. There is a linear correlation between the transition equivalence ratio at which the effectiveness switches from FSD to ASD, and the rich flammability limit for all three fuels.

Keywords: Laminar flames; Suppression; Fuel type; Partially premixed flames

1. Introduction

Our previous investigations of the extinction of CO_2-diluted methane–air partially premixed flames (PPFs) [1–3] have shown that the relative effectiveness of fuel and air stream dilution (FSD and ASD, respectively) varies significantly with the fuel stream equivalence ratio. This is significant since fire suppressants are typically introduced into the air surrounding a flame, which may not always be the most effective action for flame suppression. Herein, we investigate the effectiveness of fuel and air stream dilution with CO_2 in suppressing PPFs for various fuels. We find that the rich flammability limit of a flame has a significant impact on the effectiveness of the suppressant and on the roles of FSD and ASD.

Flames suppression by an agent can occur due to the following three effects or a combination thereof [4]: (i) the chemical effect of an agent, such as halon, which influences the flame chemistry by

* Corresponding author. Fax: +1 301 975 4052.
E-mail address: andrew.lock@nist.gov (A. Lock).

1540-7489/$ - see front matter © 2009 The Combustion Institute. Published by Elsevier Inc. All rights reserved.
doi:10.1016/j.proci.2008.05.031

reducing the concentration of key radical species, (ii) the thermal effect of an inert agent that decreases the flame temperature; and (iii) the dilution effect that decreases the concentration of a deficient reactant, thereby also decreasing the flame temperature. Halons are very effective chemically active flame suppressants [5,6]. However a ban on their production since 1994 [7], has led to the introduction of a variety of alternative suppressants [8–10], including such inert alternatives as water mist [11] and inert gases [12–14]. The effectiveness of CO_2 as a flame suppressant has been examined in different configurations [1–3,15,16] but there is no comparison available of its relative effectiveness as it is introduced into the primary fuel and primary air streams of PPFs.

We have reported experimental and numerical results for the relative effectiveness of FSD and ASD in suppressing CO_2-diluted methane–air flames [1]. We found that as the level of partially premixing is decreased for both counterflow and coflow methane–air flames, ASD is increasingly more effective as compared to FSD in suppressing the flames. Consequently, non-premixed flames (NFs) are becoming more readily extinguished by adding CO_2 to the air stream while FSD is becoming more effective in extinguishing the corresponding PPFs. Similar results for several inert and chemically active flame suppressants have been reported [17–19]. Trees suggested that the effectiveness of a suppressant in the fuel and air streams of a flame depends upon the fuel [20]. This is supported by other investigations [17–19] that showed that the relative effectiveness of fuel and air stream dilutions can change significantly for a NF as the fuel changes. Thus, a general observation from these investigations is that the dilution of either the fuel or air stream may be typically the more effective means of flame suppression for a certain condition [3,5] for both inert and chemically active agents.

The literature contains many reports on the relative effectiveness of fuel and air stream dilution in suppressing methane–air PPFs in both counterflow and coflow configurations. However, the role of fuel in determining this relative effectiveness has been examined only in the context of NFs and not for PPFs. Thus, it is important to extend these studies because unwanted fires often originate in a partially premixed mode with a variety of fuels.

Herein, we focus on the suppression of methane, ethylene, and acetylene PPFs using CO_2 as a diluent that is independently introduced into the fuel and air streams. Our objective is to examine the effect of fuel in determining the relative effectiveness of FSD and ASD in extinguishing the PPFs for coflow and counterflow flames, which also enables us to examine the effect of configuration on flame suppression.

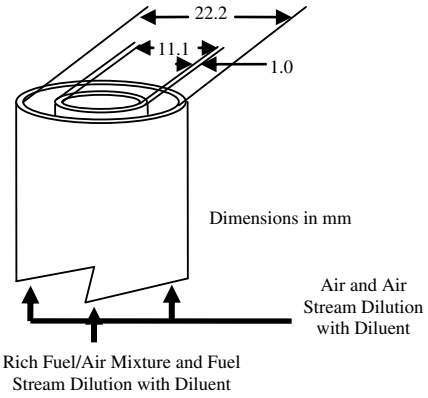

Fig. 1. A schematic of the burner. Fine mesh screens are inserted into both the central duct and annulus of the burner to provide a plug flow velocity profile.

1.1. Experimental configuration

Two-dimensional axisymmetric flames were established on a coflow burner consisting of two annular tubes that is schematically presented in Fig. 1. The inner tube has an internal diameter of 11.1 mm and a wall thickness of 1 mm while the outer tube has an ID of 22.2 mm. Several fine mesh screens are inserted into the burner annuli and placed just inside the burner exit in order to provide a plug flow exit velocity profile. For cases presented here, both the inner jet and the coflow velocities were held constant at 50 ± 0.32 cm/s (combined expanded uncertainty with a coverage factor of $k = 2$) in order to minimize shear effects on flame liftoff and blowout.

Two gas bottles supplied the diluted fuel and air stream mixtures that were prepared prior to each experiment. All fuels were laboratory grade gases (Airgas[1] CH_4 99.95%, C_2H_4, 99.95%, and C_2H_2 99.5% with trace acetone) that were burned in filtered and dried compressed air (Airgas). Premixing CO_2 (Airgas, 99.9%) with the fuel–air mixtures in the bottles prior to each experiment provided dilution. The uncertainty (expressed with a coverage factor of 2) in the composition of diluted fuel–air mixtures was less than 1%.

In our investigation, the amount of CO_2 dilution in the fuel or air stream was continuously increased for a jet flame established at a specified level of partial premixing so as to cause it to first lift off from the burner, increase its liftoff height,

[1] Certain companies and commercial properties are identified in this paper in order to specify adequately the source of information or of equipment used. Such identification does not imply endorsement or recommendation by the National Institute of Standards and Technology, nor does it imply that this source or equipment is the best available for the purpose.

and eventually extinguish it through blowout. Air stream diluted C_2H_2 flames could not be experimentally established due to safety issues pertaining to our experimental setup while partially premixed acetylene flames were burner attached regardless of the amount of ASD and produced significant heat damage to the burner. For the prescribed flow conditions, the C_2H_2 flames without fuel stream dilution were too large and sooty at high equivalence ratio cases or had relatively high flame temperatures (that caused the burner material to overheat and melt) and high flame speeds at lower equivalence ratios approaching stoichiometric (that produced flashback). FSD and ASD experiments on flames burning methane and ethylene were performed with the diluent volume fraction in the range $0 \leqslant X_{CO_2} \leqslant blowout$. Experiments for C_2H_2 flames with FSD were performed with an initially large X_{CO_2} value that produced a lifted flame. This value was progressively decreased until the flame became burner attached.

The flow was regulated by two MKS mass flow controllers with an uncertainty of 1% of full scale flow. Direct images of the flames were taken with a (640 × 480) pixel charged coupled device (CCD) camera (Sony F828). The overall uncertainty in the flame liftoff height measurements is ±5%, and arises due to buoyancy induced oscillations [2,21,22], and uncertainties in the camera location and focal length.

1.2. Numerical models

Axisymmetric coflow flames were simulated based on the algorithm developed by Katta et al. [23]. The method, which is described elsewhere in detail [24,25], solves the time-dependent governing equations for unsteady reacting flows in an axisymmetric configuration, i.e.,

$$\frac{\partial(\rho\Phi)}{\partial t}+\frac{\partial(\rho u\Phi)}{\partial z}+\frac{\partial(\rho v\Phi)}{\partial r} = \frac{\partial}{\partial z}\left(\Gamma^{\Phi}\frac{\partial\Phi}{\partial z}\right)+\frac{\partial}{\partial r}\left(\Gamma^{\Phi}\frac{\partial\Phi}{\partial r}\right)-c\frac{\rho v\Phi}{r} + c\frac{\Gamma^{\Phi}}{r}\frac{\partial\Phi}{\partial r}+S^{\Phi}.$$

Here, t denotes the time, and u and v represent the axial (z) and radial (r) velocity components, respectively. The general form of the equation represents conservation of mass, momentum, species, or energy conservation, depending on the variable used for σ. The diffusive transport coefficient Γ^{Φ} and source terms S^{Φ} appearing in the equation are provided in Table 1 of Ref. [26]. Introducing the overall species conservation equation and the state equation completes the set of equations. In addition, a sink term based on an optically thin gas assumption is included in the energy equation to account for thermal radiation from the flame [27].

Simulations employed a computational domain of 150 × 100 mm in the axial (z) and radial (r) directions with a non-uniform staggered 401 × 101 grid. The grid was produced through sequential refining of the number of points until there was negligible change in the flame shape, structure, and other characteristics. Numerical investigations establishing grid independence have been reported elsewhere [28]. The simulations employed the same burner configuration as shown in Fig. 1, with nearly flat velocity profiles at the burner exit that match our experiments. Appropriate boundary conditions were employed at the axis of symmetry, outflow (top and outer), and inflow boundaries. The outflow boundaries were situated sufficiently far from the flame to minimize their effect on the simulation. A detailed discussion of the boundary conditions is also presented elsewhere [22,28,29]. The methane–air chemistry is modeled using a detailed mechanism that considers 24 species and 81 elementary reactions [30]. This mechanism has been extensively validated for the computation of premixed flames speeds and the detailed structures of non-premixed and partially premixed methane–air flames [26,31–33]. The ethylene–air and acetylene–air flames were simulated using the GRI-Mech 1.2 mechanism [34], since this mechanism yielded better agreement with experiments for these fuels.

The counterflow methane–air, ethylene–air, and acetylene–air flames were simulated using the OPPDIFF code [35]. The separation distance between the two opposed nozzles was 2.54 cm. The fuel and oxidizer temperatures were assumed to be 300 K. The global strain rate $a_s = 2|V_2|/l\left[1+\left(|V_1|\sqrt{\rho_1}/|V_2|\sqrt{\rho_2}\right)\right]$ was maintained at $a_s = 200\ s^{-1}$ [36]. The momenta of the two jets were adjusted to locate the flame close to the center of the flowfield. Grid independence of the results was achieved by adjusting the values of the GRAD and CURV parameters and using adaptive re-gridding to resolve the structures of both the premixed and non-premixed reaction zones. Mixture averaged transport properties were used for all simulations and negligible differences were observed in comparison with the multi-component transport model. The flame chemistry for all three fuels in the counterflow configuration was modeled using the GRI-Mech 3.0 mechanism [34]. Validation results are presented in the next section. As shown in Fig. 2, there are negligible differences in the flame structures predicted using the GRI-1.2 and GRI-3.0 mechanisms.

2. Results and discussion

2.1. Validation of numerical model

Figure 2 presents a comparison of our predictions using the GRI-1.2 (solid) and GRI-3.0

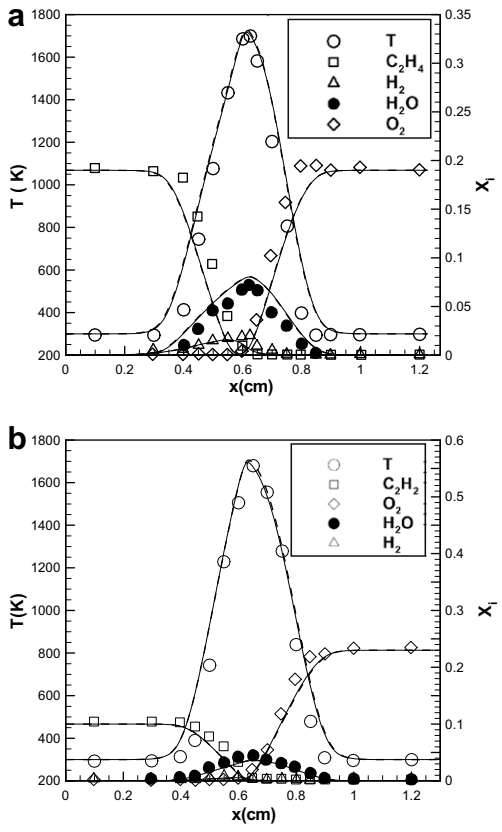

Fig. 2. Comparison of the predictions, using the GRI-Mech 1.2 (solid lines) and 3.0 (dashed) mechanisms, with the measurements of Sun and Law for N_2 diluted ethylene (a) and acetylene (b) non-premixed counterflow flames established at a strain rate of $a_s = 56\ s^{-1}$.

(dashed) mechanisms with previous measurements [37] for counterflow N_2-diluted, non-sooting C_2H_4 and C_2H_2 flames. The flame structure is presented in terms of temperature and H_2, O_2, H_2O, and C_2H_4 (or C_2H_2) volume fraction profiles. There are negligible differences between the predictions and measurements, implying that the differences between the mechanisms in terms of the critical CO_2 volume fraction for flame extinction are also expected to be small. For additional validation, we computed the critical CO_2 volume fractions X_{CO_2} for the extinction of fuel and air stream diluted non-premixed methane–air flames established at $a_s = 100\ s^{-1}$, and compared them with previous measurements [15]. Our predicted CO_2 volume fractions for the extinction of fuel and air stream diluted flames are $X_{CO_2} = 0.71$ and $X_{CO_2} = 0.14$, respectively, while the corresponding measured values were $X_{CO_2} = 0.70$ and $X_{CO_2} = 0.14$, respectively, providing further validation of the simulations.

The two dimensional (2-D) axisymmetric computational model that we employ for coflow flames has been previously validated against experimental data for a variety of steady and unsteady laminar methane–air flames, including opposed-jet diffusion flames [16], burner-stabilized [24,32,38] and lifted flames [16,39], and 1-g and microgravity flames [2,16,32,40,41]. Figure 3 presents additional validation by comparing the predicted heat release rate contours with the measured luminosity images for CO_2-fuel stream diluted ethylene and acetylene partially premixed flames established at $\phi = 2.0$ and $X_{CO_2} = 0.40$. There is generally good agreement between predictions and measurements in terms of the flame topology including the locations of the various reaction zones, rich premixed (RP), lean premixed (LP), and non-premixed (NP), and liftoff heights for C_2H_4 and C_2H_2 flames.

2.2. Coflow flame liftoff and blowout characteristics

Figure 3 presents the measured visual images, resulting from chemiluminescense and soot radiation, and predicted heat release rate contours for FSD C_2H_4 and C_2H_2 flames established at $\phi = 2.0$ with $X_{CO_2} = 0.40$. For these conditions the CH_4 flame is extinguished. For all three fuels, a PPF structure is observed in both experiments and simulations as indicated by the multiple reaction zones. Methane–air flames also exhibit a PPF structure prior to extinction. The figure illustrates the differences between the liftoff and blowout characteristics of CH_4, C_2H_4, and C_2H_2 flames established under similar conditions. For the same

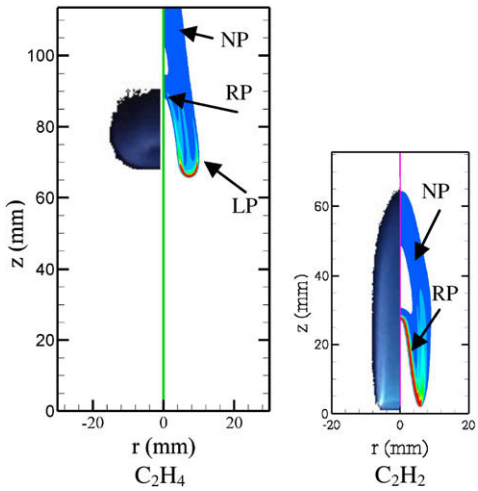

Fig. 3. Measured luminous images and predicted heat release rate contours for CO_2-fuel stream diluted (FSD) C_2H_4 and C_2H_2 flames established at $\phi = 2.0$ and with $X_{CO_2} = 0.4$. The CH_4 flame at these conditions is extinguished.

dilution and stoichiometric conditions, the CH_4 flame is extinguished through blowout; the C_2H_4 flame is considerably weakened through dilution and established far downstream from the burner rim; and the C_2H_2 flame is burner attached. Thus, irrespective of the level of partial premixing, CH_4, C_2H_4, and C_2H_2 flames become increasingly more difficult to extinguish as the C/H ratio is increased. This is consistent with previous experimental studies on flame suppression that used both chemically active and inert diluents [17–19].

In order to examine the effect of fuel type on flame liftoff and blowout (or extinction), the diluted CH_4, C_2H_4, and C_2H_2 coflow flames were established at a specified level of partial premixing and the amount of CO_2 dilution in the fuel or air streams was gradually increased to cause flame liftoff from the burner and subsequent extinguishment through blowout. Measurements included images of burner-stabilized and lifted flames (cf. Fig. 3) and their liftoff heights. For sake of brevity, the flame images are not provided here, and can be found in Ref. [42]. Figure 4 presents liftoff heights plotted with respect to the CO_2 volume fraction for FSD ethylene and acetylene flames established at different fuel-side equivalence ratios ϕ (for NFs $\phi = \infty$). The corresponding results for methane flames have been previously reported [1,3,42].

There is good agreement between the predicted and measured liftoff heights for the various levels of dilution and partial premixing, providing further validation for the computational and flame chemistry models. Both experiments and simulations indicate that as the amount of dilution increases, flames that are initially attached at the burner rim first slowly liftoff, then move away rapidly from the burner, with blowout occurring at a critical CO_2 volume fraction. The effect of partial premixing on the flame liftoff and blowout behavior is qualitatively similar for all fuels. In general, as the level of partial premixing is increased (i.e., ϕ is decreased), flames become increasingly more sensitive to FSD. However, this behavior may not be present for $\phi < 1$. Therefore, irrespective of the fuel burned, PPFs ($\phi > 1$) liftoff more easily and blowout at a lower CO_2 volume fraction as compared to the corresponding NFs.

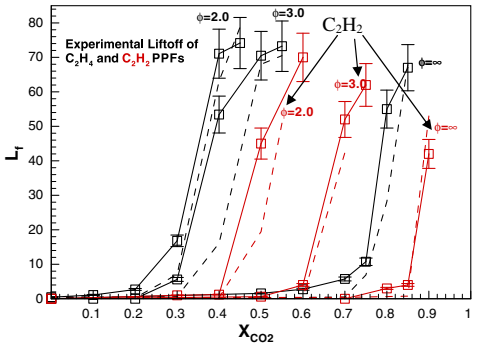

Fig. 4. Measured (symbols) and predicted (lines) liftoff heights of FSD C_2H_4 and C_2H_2 PPFs plotted versus X_{CO_2} for different equivalence ratios.

For similar conditions, the flames are increasingly more difficult to extinguish as they burn (in the order) methane, ethylene, and acetylene. Thus, for the same level of partial premixing, the critical CO_2 volume fractions required for the liftoff and blowout of acetylene flames are the highest, with the lowest required for the corresponding methane flames. This is consistent with the highest adiabatic flame temperatures and laminar flame speeds for acetylene–air mixtures and lowest ones for methane–air mixtures. Moreover, the flammability limits of acetylene–air mixtures ($0.27 < \phi < 68$) are significantly wider than those of ethylene–air mixtures ($0.4 < \phi < 8$), which are in turn wider than those for methane–air mixtures ($0.5 < \phi < 1.7$) [36].

2.3. Global blowout (extinction) characteristics of coflow and counterflow flames

As stated earlier, due to their high flame temperatures, wide flammability limits, and high flame speeds, acetylene flames could not be established using ASD in our experimental setup. In contrast, there was no difficulty in establishing ethylene flames in the burner-stabilized and lifted modes. However, these flames could not be extinguished using ASD even with $X_{CO_2} = 1$ in the air stream, due to their wide flammability limits, the lower CO_2 diffusivity in fuel as compared to its diffusion in air, and the presence of oxygen in the ambient air outside the outer annular jet which precluded a "total flooding" condition. Consequently, in order to characterize the influence fuel type on the extinction of ASD flames, we simulated counterflow CH_4, C_2H_4, and C_2H_2 flames and examined their behavior. Our focus was on diluted flames near extinction at relatively large strain rates ($a_s = 200\ s^{-1}$) where sooting was not an issue.

Figure 5 presents the extinction/blowout characteristics for several fuel and air stream diluted CH_4, C_2H_4, and C_2H_2 flames in the counterflow and coflow configurations. For each case, the critical CO_2 volume fraction required for flame extinction is plotted with respect to the inverse equivalence ratio (ϕ^{-1}). The salient observations follow.

1. There is generally good agreement between simulations and experiments in terms of the critical CO_2 volume fraction (X_{CO_2}) for flame extinction for different levels of partial premixing. Irrespective of the fuel burned, as the level of partial premixing is increased (i.e., ϕ^{-1}

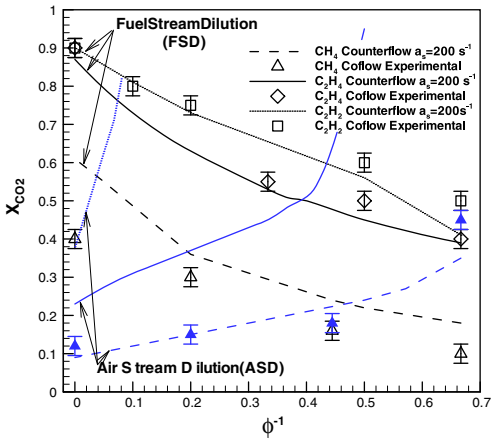

Fig. 5. Critical diluent mole fraction X_{CO_2} required for the extinction of fuel (FSD) and air stream diluted (ASD) CH_4, C_2H_4, and C_2H_2 coflow and counterflow flames (established at $a_s = 200\ s^{-1}$) plotted versus ϕ^{-1}. The black lines (simulations) and symbols (measurements) indicate FSD results and the blue lines and symbols indicate ASD results. (For interpretation of color mentioned in this figure the reader is referred to the web version of the article.)

increased), X_{CO_2} decreases for FSD while it increases for ASD. This suggests that FSD becomes more effective and ASD less effective as the flame becomes more partially premixed. Consequently, NFs are generally more sensitive to ASD, while PPFs are more sensitive to FSD, implying that dilution of the deficient reactant stream is typically the more effective means of flame suppression.

2. The extinction/blowout behavior presented in terms of different dilutions, partial premixing and burner configuration is qualitatively similar for all three fuels. There are, however, significant quantitative differences attributable to the fuel used. Again, for the same conditions, both FSD and ASD flames are increasingly more difficult to extinguish in the order methane, ethylene, and acetylene.
3. There is good correspondence between the extinction of counterflow and coflow flames for all fuels, particularly for FSD flames. For all fuels, there is good agreement between the critical volume fraction X_{CO_2} required for the extinction of FSD counterflow and coflow flames. As the level of partial premixing is increased, the critical X_{CO_2} value decreases, i.e., FSD is more effective as the flames become more partially premixed. This similarity is interesting since the counterflow flame extinction occurs through dilution and thermal effects that decrease the flame temperature, while coflow flame extinction also involves aerodynamic effects that cause flame liftoff and subsequent transition to a triple flame structure.
4. For ASD flames, there are noticeable differences between the extinction behavior of counterflow and coflow flames implying that aerodynamic effects can be significant. These effects are more prominent for C_2H_4 and C_2H_2 flames than for CH_4 flames. For counterflow flames, there is a transition equivalence ratio ϕ_{tr}; FSD is more effective when $\phi < \phi_{tr}$ while the effectiveness of ASD is greater when $\phi_{tr} < \phi\infty$. The value of ϕ_{tr} increases as the fuel C/H ratio increases – $\phi_{tr} \approx 2.0$, 3.3 and 13.0 for CH_4, C_2H_4 and C_2H_2 flames (cf. Fig. 5), respectively. In contrast, for coflow flames, this transition is observed only for CH_4, flames; the computed and measured $\phi_{tr} \approx 2.0$. For the conditions investigated, C_2H_4 and C_2H_2 coflow flames cannot be extinguished using ASD as discussed earlier. Consequently, the effects of configuration and fuel type become more significant for ASD flames.

In order to further elucidate ASD and FSD suppression, we plot the peak flame temperature T_{max} as a function of X_{CO_2} for counterflow flames in Fig. 6. The behavior of C_2H_2 flames is qualitatively similar to those for C_2H_4 flames (and is therefore not included for the sake of brevity), while that of CH_4 flames has been previously reported [1]. With FSD, flame suppression is achieved at any equivalence ratio for all three fuels, while using ASD flame suppression depends strongly on the fuel and level of partial premixing.

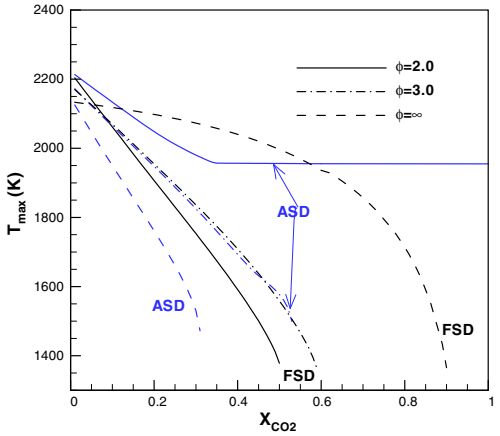

Fig. 6. Flame temperature T_{max} plotted versus with X_{CO_2} for C_2H_4 counterflow flames established at $\phi = 2.0$ (solid lines), $\phi = 3.0$ (dashed dotted lines), and ∞ (dashed lines) for $a_s = 200\ s^{-1}$ with FSD (black lines) and ASD (blue lines). (For interpretation of color mentioned in this figure the reader is referred to the web version of the article.)

For CH_4 flames, ASD leads to flame suppression at all ϕ values for PPFs and NFs [cf. Fig. 7 in Ref. [1]]. However, for C_2H_2 and C_2H_4 flames, ASD leads to flame suppression only when $\phi > 2$ for C_2H_4 flames, and $\phi > 10$ for C_2H_2 flames.

As shown in Fig. 6 for $\phi = 2.0$, as X_{CO_2} in the air stream is increased, T_{max} first decreases and then becomes constant as X_{CO_2} is further increased. This indicates that the non-premixed reaction zone of the C_2H_4 PPF first cools but as X_{CO_2} is increased ASD becomes far less effective in suppressing the premixed zone. A similar behavior is observed for C_2H_2 flames except that the inability to suppress the flame with ASD expresses itself when $\phi < 10$. The larger value of ϕ in this case is due to its higher rich flammability limit.

2.4. Correlation between transition equivalence ratio and flammability limit

We now examine the transition equivalence ratio more closely. Based on our previous analysis [3,42], for $\phi < \phi_{tr}$, the fuel is the deficient reactant while for $\phi_{tr} < \phi < \infty$, the oxidizer is deficient (cf. Fig. 5). The value of ϕ_{tr} for the three fuels increases in the order CH_4, C_2H_4, and C_2H_2. Since the rich flammability limit ϕ_R for the three fuels also increases in the same order, we hypothesize that there is a correlation between ϕ_{tr} and ϕ_R. Figure 7 presents a plot of ϕ_{tr} as a function of ϕ_R of the three fuels for which a regression analysis yields: $\phi_{tr} = 0.16\phi_R + 1.73$. Thus, the relative effectiveness of FSD and ASD scales with the fuel flammability limit, since FSD moves flames towards the lean limit and ASD towards the rich limit. ASD does not produce significant flame suppression below a certain ϕ value since it can only move the fuel–air mixture to its inflow composition but not richer than that.

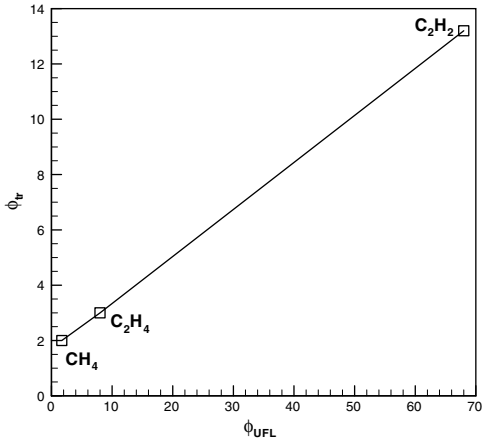

Fig. 7. Variation of transition equivalence ratio (ϕ_{tr}) verses equivalence ratio (ϕ_R) corresponding to the upper flammability limit of a fuel.

3. Conclusions

Experimental measurements and numerical predictions are presented to elucidate differences in the extinction behavior of CH_4, C_2H_4, and C_2H_2 coflow jet and counterflow flames with CO_2 dilution of the primary fuel and primary air streams. Laboratory experiments are supplemented with 2-D and 1-D counterflow simulations. Important observations include:

1. CH_4, C_2H_4, and C_2H_2 require sequentially larger X_{CO_2} values to liftoff and extinguish. Thus, both FSD and ASD suppression becomes increasingly less effective in the order for flames established with C_2H_4, C_2H_2 and CH_4. PPFs are generally more easily extinguished by FSD while NFs are more readily extinguished through ASD.
2. There is good correspondence between the extinction of counterflow and coflow flames for all fuels, particularly for FSD flames. Counterflow CH_4, C_2H_4 and C_2H_2 flame extinction with CO_2 FSD agrees with the corresponding coflow suppression.
3. There are more significant differences between the extinction behavior of ASD counterflow and coflow flames. ASD extinction of C_2H_4 and C_2H_2counterflow flames is observed only in the certain range of equivalence ratios, while ASD is unable to significantly suppress C_2H_4 or C_2H_2 coflow flames due to the effects of buoyancy, aerodynamics, and the wider fuel flammability limits.
4. The effectiveness of FSD and ASD transitions at different equivalence ratios for the three fuels. This transition is attributed to the dilution of the deficient reactant, and shown to correlate with the fuel flammability limit.

References

[1] A. Lock, A. Briones, S.K. Aggarwal, I.K. Puri, U. Hegde, *Combust. Flame* 149 (4) (2007) 340–352.
[2] A. Lock, A. Briones, X. Qin, S.K. Aggarwal, I.K. Puri, U. Hegde, *Combust. Flame* 143 (3) (2005) 159–173.
[3] A. Lock, S.K. Aggarwal, I.K. Puri, U.G. Hegde, *Fire Saf. J.* 43 (1) (2008) 24–35.
[4] K.Y. Lee, D.J. Cha, A. Hamins, I.K. Puri, *Combust. Flame* 104 (1–2) (1996) 27–40.
[5] G.R. Gann, in: G.R. Gann (Ed.), *Halogenated Fire Suppressants*, ACS Symposium Series Washington, DC, 1975.
[6] B.A. Williams, J.W. Fleming, *Proc. Combust. Inst.* 29 (2003) 345–351.
[7] UNEP Montreal Protocol on Substances that Deplete the Ozone Layer, 1992.
[8] G.T. Linteris, D.R. Burgess, V. Babushok, M. Zachariah, W. Tsang, P. Westmoreland, *Combust. Flame* 113 (1–2) (1998) 164–180.

[9] G.T. Linteris, V.R. Katta, F. Takahashi, *Combust. Flame* 138 (1–2) (2004) 78–96.
[10] G.T. Linteris, L. Truett, *Combust. Flame* 105 (1–2) (1996) 15–27.
[11] R. Seiser, K. Seshadri, *Proc. Combust. Inst.* 30 (2005) 407–414.
[12] L. Qiao, C.H. Kim, G.M. Faeth, *Combust. Flame* 143 (1–2) (2005) 79–96.
[13] N. Saito, Y. Ogawa, Y. Saso, C.H. Liao, R. Sakei, *Fire Saf. J.* 27 (3) (1996) 185–200.
[14] R.S. Sheinson, J.E. Pennerhahn, D. Indritz, *Fire Saf. J.* 15 (6) (1989) 437–450.
[15] M. Bundy, A. Hamins, K.Y. Lee, *Combust. Flame* 133 (3) (2003) 299–310.
[16] V.R. Katta, F. Takahashi, G.T. Linteris, *Combust. Flame* 137 (4) (2004) 506–522.
[17] E.C. Creitz, *J. Res. Natl. Bur. Stds.* 65 (4) (1961).
[18] R.F. Kubin, R.H. Knipe, A.S. Gordon, *Halog. Fire Suppress.* 16 (1975).
[19] T. Niioka, T. Mitani, M. Takahashi, *Combust. Flame* 50 (1983) 89–97.
[20] D. Trees, A. Grudno, K. Seshadri, *Combust. Sci. Technol.* 124 (1–6) (1997) 311.
[21] S.K. Aggarwal, I.K. Puri, *AIAA J.* 36 (7) (1998) 1190–1199.
[22] X. Qin, I.K. Puri, S.K. Aggarwal, *Proc. Combust. Inst.* 29 (2002) 1565–1572.
[23] V.R. Katta, L.P. Goss, W.M. Roquemore, *Combust. Flame* 96 (1–2) (1994) 60–74.
[24] R. Azzoni, S. Ratti, S.K. Aggarwal, I.K. Puri, *Combust. Flame* 119 (1–2) (1999) 23–40.
[25] A.J. Lock, R. Ganguly, I.K. Puri, S.K. Aggarwal, U. Hegde, *Proc. Combust. Inst.* 30 (2005) 511–518.
[26] Z. Shu, S.K. Aggarwal, V.R. Katta, I.K. Puri, *Combust. Flame* 111 (4) (1997) 296–311.
[27] R. Siegel, J. Howell, *Thermal Radiation Heat Transfer*, Taylor and Frances, 2002.
[28] A.M. Briones, S.K. Aggarwal, V.R. Katta, *Phys. Fluids* 18 (4) (2006).
[29] Z. Chen, X. Qin, B. Xu, Y.G. Ju, F.S. Liu, *Proc. Combust. Inst.* 31 (2) (2006) 2693–2700.
[30] N. Peters, B. Rogg, *Reduced Kinetic Mechanisms for Applications in Combustion SystemsLect. Notes Phys.*, vol. m15, Springer-Verlag, 1993.
[31] S.K. Aggarwal, I.K. Puri, X. Qin, *Phys. Fluids* 13 (1) (2001) 265–275.
[32] R. Azzoni, S. Ratti, I.K. Puri, S.K. Aggarwal, *Phys. Fluids* 11 (11) (1999) 3449–3464.
[33] H.S. Xue, S.K. Aggarwal, *AIAA J.* 39 (4) (2001) 637–645.
[34] G.P. Smith, D.M. Golden, M. Frenklach et al., in: Internet: <http://www.me.berkeley.edu/gri_mech/>.
[35] R.J. Kee, F.M. Rupley, J.A. Miller et al., in: *Reaction Design*, 2004.
[36] K.K. Kuo, *Principles of Combustion*, John Wiley and Sons, New Jersey, 2005.
[37] C.J. Sun, C.J. Sung, H. Wang, C.K. Law, *Combust. Flame* 107 (4) (1996) 321–335.
[38] Z. Shu, B. Krass, C. Cho, S.K. Aggarwal, V. Katta, I.K. Puri, *Proc. Combust. Inst.* 27 (1998) 625.
[39] B.J. Lee, S.H. Chung, *Combust. Flame* 109 (1–2) (1997) 163–172.
[40] A. Lock, R. Ganguly, I.K. Puri, S.K. Aggarwal, *Proc. Combust. Inst.* 30 (30) (2004) 511–518.
[41] F. Takahashi, W.J. Schmoll, V.R. Katta, *Proc. Combust. Inst.* 27 (1998) 675.
[42] A. Lock. *Extinction of Fuel and Air Stream Diluted Partially Premixed Flames for Fire Safety*, University of Illinois at Chicago, Chicago, IL, 2007.